Cha *et al. J Wood Sci* (2020) 66:28
https://doi.org/10.1186/s10086-020-01875-2

Journal of Wood Science

ORIGINAL ARTICLE Open Access

Effect of temperature on the mechanical performance of plywood used in membrane-type LNG carrier insulation systems

Seung-Joo Cha[1], Jeong-Dae Kim[1], Seul-Kee Kim[1], Jeong-Hyeon Kim[1], Hoon-Kyu Oh[2], Yong-Tai Kim[2], Seong-Bo Park[2] and Jae-Myung Lee[1*]

Abstract

In this study, the mechanical performance of melamine–urea–formaldehyde (MUF) resin plywood composed of an orthotropic material, which is used as a structural material in liquefied natural gas (LNG) cargo containment systems (CCSs), is evaluated. With a decrease in temperature, the plywood changes from ductile to brittle under compressive loads; thus, it may fail to distribute the compressive loads caused by sloshing impact as well as lose its stiffness, which helps maintain the shape of the structure. However, only a few studies investigated the mechanical characteristics of MUF resin plywood under compressive loads caused by sloshing impact as well as the crack propagation and change in material features with decreasing temperatures. Therefore, the present study investigated the mechanical performance of MUF plywoods of different thicknesses under different temperatures and grain orientation parameters. The results indicate the mechanical properties of MUF plywood for compression with decreasing temperatures. Furthermore, based on thermomechanical analysis, this study shows that the critical temperature at which the plywood material tends to transition from ductile to brittle behavior is − 110 °C. This finding will help in the design of MUF plywood-based LNG CCSs considering its low-temperature brittleness.

Keywords: Liquefied natural gas, Plywood, Fracture behavior, Mechanical properties, Ultimate strain, Fracture strain, Thermomechanical analyzer

Introduction

In the past few years, the liquefied natural gas (LNG) trade has gradually increased. The international LNG trade had rapidly grown in the 4 consecutive years since 2010 and increased by 35.2 million tons (MT) in 2017. This is because Sabine Pass Liquefaction, USA, acquired new liquefaction trains, which increased the production output at its liquefaction plant in Australia [1]. Over the past decades, the LNG shipbuilding segment has been greatly affected by the growing LNG market. This also significantly affected the LNG carrier demand and increased research interest in LNG cargo containment systems (LNG CCSs).

Among the different LNG CCSs, membrane-type CCSs are widely used because they can accommodate a large amount of liquid cargo. These membrane-type systems include Mark-III and NO96 designed by Gaztransport & Technigaz (GTT) [2], as shown in Fig. 1. They are generally composed of primary barriers, insulation panels, and secondary barriers; however, the materials are different. In the case of Mark-III, the primary barrier uses corrugated STS304L (austenitic stainless steel) to prevent

*Correspondence: jaemlee@pusan.ac.kr
[1] Department of Naval Architecture and Ocean Engineering, Pusan National University, Jangjeon-Dong, Geumjeong-Gu, Busan 609-735, South Korea
Full list of author information is available at the end of the article

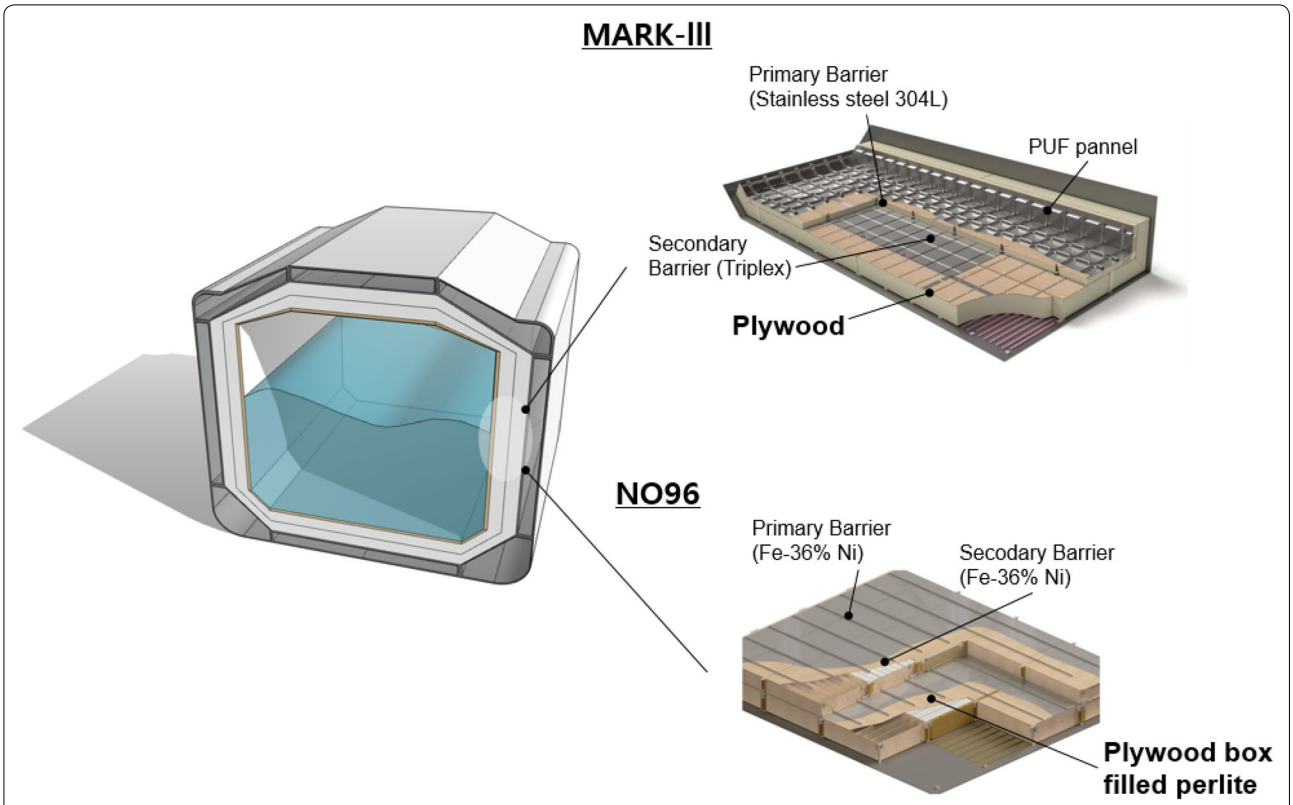

Fig. 1 GTT membrane-type LNG cargo containment system: **a** NO96 and **b** Mark-III

thermal deformation at cryogenic temperatures. The insulation panel is composed of polyurethane foam (PUF) and plywood, and the secondary barrier called a triplex consists of a metal composite sheet sandwiched between two insulation layers. In the case of NO96, the primary and secondary barriers consist of 36% nickel steel alloy (Invar steel), and the insulation panel is composed of a plywood box filled with perlite [3]. The plywood used in LNG CCSs consists of thin layers of an orthotropic material, which makes it a very strong and durable composite [4]. NO96 and Mark-III use 9-mm and 12-mm plywoods with light weight and high rigidity as structural materials [5]. The mechanical properties of the plywood are greatly affected by the fiber direction. Therefore, fiber orientation was considered in the present study [6].

Much research has been conducted on plywood in the past because it has a wide range of applications such as a building material. In particular, many studies have been conducted at room temperature and high temperatures which are often used [7, 8]. LNG CCSs are exposed to a wide range of temperatures, from room temperature to low temperatures and even cryogenic temperatures. However, there are only a few studies on LNG CCSs in extreme environments. In addition, LNG CCSs are continuously subjected to sloshing impact loads during operation, which can cause fracture due to bending, tension, and compression loads. Therefore, the mechanical testing of the insulation is imperative to maintain the safety of the LNG CCSs. Kim et al. [5, 9] investigated the effects of cryogenic temperature and thermal treatment on the mechanical characteristics of melamine–urea–formaldehyde (MUF) resin plywood through bending and tensile tests. They also performed a comparative study of phenolic-formaldehyde (PF) and MUF resins regarding the effects of temperature, grain orientation, and thermal treatment. The results revealed the effectiveness of MUF resin plywood, whose mechanical strength is higher than that of conventional PF resin plywood under ambient and cryogenic temperatures. Arswendy and Moan [10] conducted failure analysis (crushing and buckling) of plywood bulkheads at ambient temperature. The buckling tests results were compared with finite element analysis (FEA) results to determine the maximum buckling capacity of the plywood bulkhead. Besides, Choi et al. [11] and Ivanov and Sadowski [7] performed tensile tests to confirm the effect of tensile and buckling load. Although a few studies have been conducted on the compression properties of plywood at ambient temperature [12, 13], the compression properties at cryogenic temperatures have been rarely investigated. MUF resin plywood

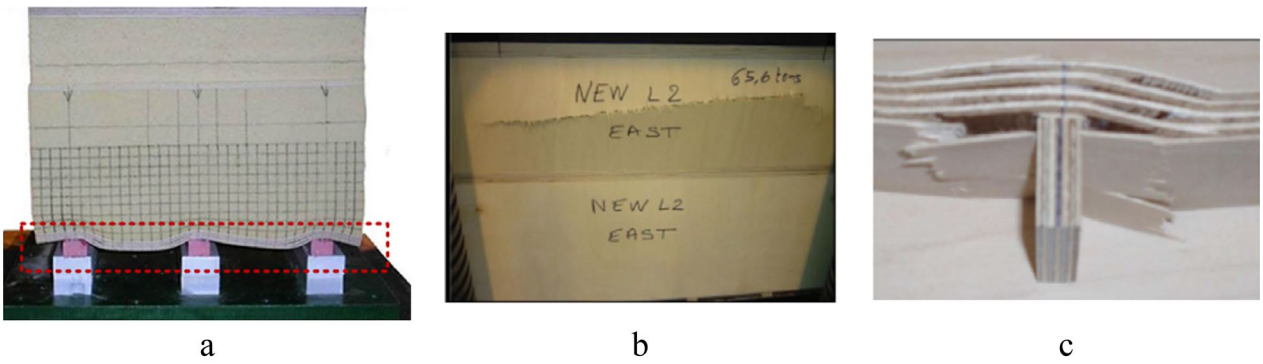

Fig. 2 Photographs of the failure characteristics of GTT membrane-type LNG cargo containment system caused by compressive load: **a** buckling and crushing of Mark-III [5], **b** buckling of primary bulkhead of NO96 [20], and **c** fracture of primary cover plate of NO96 [20]

has better mechanical strength than the PF resin plywood used LNG CCSs. Moreover, MUF resin has a short fabrication time, is water resistant, and reduce formaldehyde emissions; however, MUF resin plywood needs to gain reliability for the low temperature brittleness [14]. There is insufficient data regarding the compressive behavior of MUF resin plywood at cryogenic temperatures, which limits its application in LNG CCSs. Thus, this study investigated the fracture behavior of MUF resin plywood by compressive behavior occurred in LNG CCSs. As shown in Fig. 2, the impact load due to liquid cargo sloshing causes an additional load on the plywood of Mark-III and NO96. In the case of Mark-III, plywood has a role to prevent the local load for polyurethane foam by compressive load occurred in the vertical direction of the plywood. In the case of NO96 composed of plywood having a grid structure, compressive load occurs in the vertical direction as well as perpendicular to the grain direction [10, 11, 15]. In other words, the compressive load on the plywoods in NO96 and Mark-III caused by the sloshing impact is complex and repetitive, and is an important load factor in the design of insulation for LNG CCSs [16]. The exposure to extreme environments such as sloshing impact and cryogenic temperatures can cause micro-cracks in LNG CCSs, leading to the failure of the laminated sandwich structure [17]. Therefore, it is necessary to identify the micro-cracks.

In this study, the compressive behavior of MUF resin plywood (with 9 mm and 12 mm thicknesses) used in NO96 and Mark-III was investigated considering the actual compressive environment of LNG CCSs involving sloshing impact at a wide range of temperatures (from ambient to cryogenic temperatures) [18, 19]. The compression tests were performed in longitudinal and transverse directions as well as vertical fiber direction from room temperature to cryogenic temperature. This experimental study investigated the mechanical properties of MUF resin plywood macroscopically and microscopically and predicted the crack propagation that occurs at low temperatures to address the issue of low-temperature brittleness.

Table 1 Plywood parameters for the experiment

Veneer dimensions	1200 mm × 2400 mm × 2 mm
Veneer moisture contents	8–12%
Resin spreading rate	155 g/m^2
Bulk density	680 kg/m^3

Table 2 Size tolerances

Length/width	Tolerance
1000–2000 mm	± 2 mm
Squareness	± 0.1% or 1 mm/m
Edge straightness	± 0.1% or 1 mm/m

Experiment

Specimens

In the present study, MUF resin-bonded plywood specimens with 9 mm and 12 mm thicknesses were prepared to investigate the mechanical performance of the plywood. The birch plywood specimens used in this study were obtained directly from the Mark-III and NO96 LNG CCSs. Commercially produced seven-layer birch plywood panels with 9 mm and 12 mm thicknesses were supplied by Dong Sung Finetec. The plywood parameters for this experiment are listed in Table 1. The size and continuity of specimens were measured in accordance with standard EN 324 [21]. The plywood size and squareness tolerances met the requirements of standard EN 315 [22], as shown in Table 2. The thickness also fulfilled the EN 315 requirements and were in part tighter than the

standard, as shown in Table 3. MUF resin was obtained through copolymerization by mixing pre-formed urea–formaldehyde (UF) and melamine–formaldehyde (MF) resins. The relative melamine:urea mass proportion in this study was approximately 50:50. The MUF resin was synthesized with a formaldehyde/(urea and melamine) mole ratio of 1.5 and had a pH of 7.9 and 50 ± 1% solid content. The main physical parameters of the MUF resin, namely viscosity and specific gravity, were 350 mPa s and 1.2, respectively.

Figure 3 shows the schematic diagram of the different grain orientations of the plywood specimen used in the compression test. As shown, the test specimen is an orthogonally oriented material with 0° (the same direction) and 90° (vertical direction) fiber orientations and an odd number of layers. In the present study, the test specimens were prepared according to the ISO604 standard [23].

Figure 4 shows the shape and dimensions of the plywood specimens having a thickness of 9 and 12 mm used in the compression test. The flat plywood panel was machined into small compression test specimens having uniform mechanical properties. The test specimens were 25 mm × 25 mm × 9 mm and 25 mm × 25 mm × 12 mm (width × length × thickness) in size. The resin used in plywood for adhesive bonding was MUF resin. MUF resin is cheaper than PF resin as it is economical owing to its short processing time. In addition, the compressive strength of MUF resin is similar to that of PF resin and it is mainly used as an alternative to PF resin adhesive. Moreover, MUF resin overcomes the shortcomings of PF resin because of its low formaldehyde emission and high water resistance [14].

Table 3 Thicknesses, structures and thickness of the panels

Normal thickness (mm)	Number of piles (pcs)	Thickness		Weight (kg/m^2)
		Min. (mm)	Max. (mm)	
9	7	8.8	9.5	6.1
12	9	11.5	12.5	8.2

Testing method

In the present study, the compression tests were performed at 25, −20, −65, −110, and −165 °C depending on the fiber direction as shown in Table 4. The compression test was performed with a controlled strain of 1/10th the dimensions of the test specimen per minute according to ISO604. To take into account the thermal equilibrium conditions of the test specimen, a preliminary cooling was performed for approximately 1 h while maintaining the target temperature inside the chamber. Five iterations of the test were performed to obtain reliable test results.

Testing apparatus

Figure 5 shows the schematic diagram of the compression test machine. The test environment was implemented using a cryogenic chamber with a universal testing machine (UTM) for composite materials. The test was conducted using this equipment at room temperature, low temperature, and cryogenic temperature depending on the fiber direction. The relative humidity in the

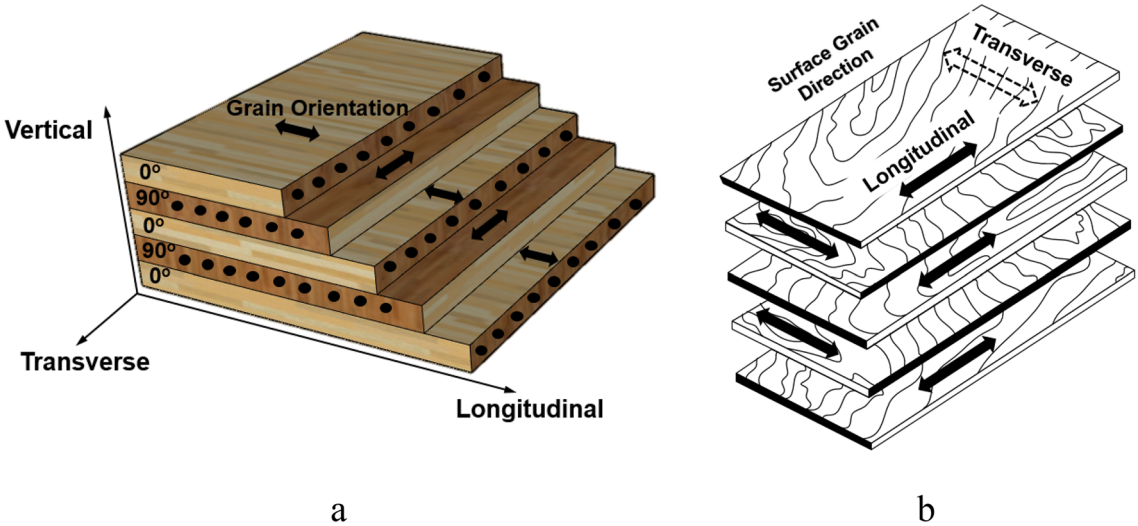

Fig. 3 **a** Photograph of the plywood compression specimen and **b** schematic diagram of the plywood panels with differing grain orientations

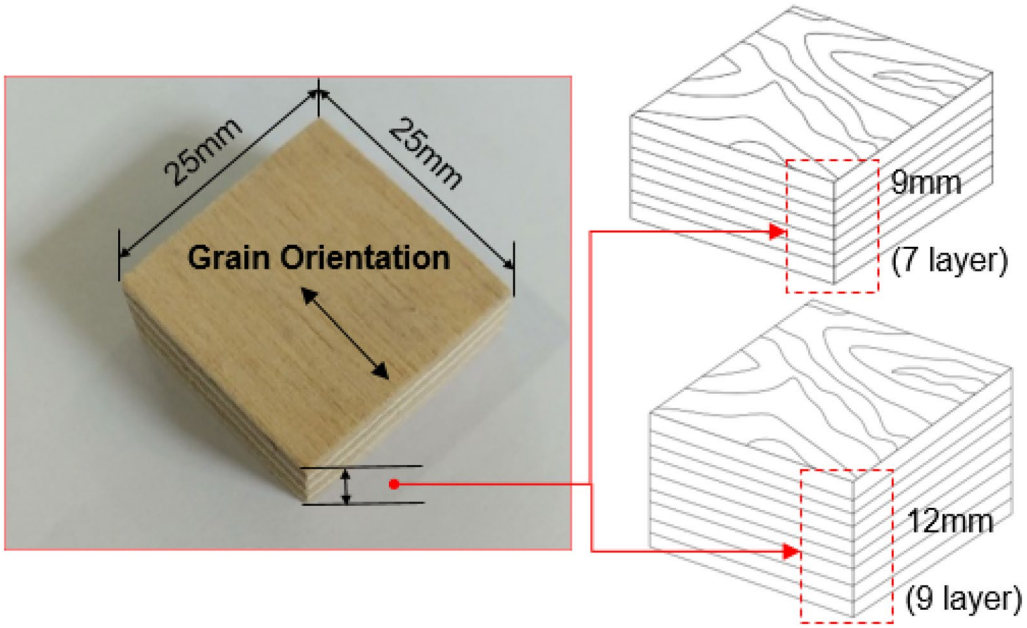

Fig. 4 Shape and dimensions of plywood test specimen

Table 4 Compression test conditions for compressed laminated wood

Material	Temperature (°C)	Number of specimens tested (loading direction)		
		(Longitudinal)	(Transverse)	(Vertical)
Plywood (9t, 12t)	25	5	5	5
	−20	5	5	5
	−65	5	5	5
	−110	5	5	5
	−165	5	5	5

compression test was approximately 45 ± 2%, in accordance with conditions defined by the ISO604 standard.

To measure the linear thermal expansion coefficient of the plywood samples, thermomechanical analysis (TMA) was conducted and thermomechanical analysis (TMA) was performed by KAIST Analysis Center for Research Advancement (KARA). The humidity of the argon used for the TMA was 0.00005% (0.5 ppm). Figure 6 shows the schematic diagram of the thermomechanical analyzer (Netzsch, TMA402) used for measuring the thermal expansion coefficient of the plywood. The thermal expansion coefficient was measured under a continuously decreasing temperature regime at a rate of 5°/min according to ASTM E831 [24]. The size of the specimen is 9 mm in cross section and 12 mm in height, and the extent to which the length of the specimen decreased with decreasing temperature over the examined temperature range (from room temperature to −150°) was measured. According to ASTM E831, the differential linear expansion coefficient (α) is calculated as the expansion coefficient of the three dimensions with a change in temperature at a constant pressure as follows:

$$\alpha = \frac{(\mathrm{d}L)_p}{(\mathrm{d}T)_p} \times \frac{1}{L_0} = \frac{(\mathrm{d}L/\mathrm{d}t)_p}{(\mathrm{d}T/\mathrm{d}t)_p} \times \frac{1}{L_0}, \quad (1)$$

where L_0 is the reference length at room temperature, T_0, on the measuring axis; L is the length at the temperature on the measuring axis; dL is the change in length over a time interval, dt, at a constant pressure; and dT is the temperature change over a time interval, dt, at a constant pressure.

Results and discussion

Mechanical performance: longitudinal and transverse direction

Figure 7 shows the longitudinal and transverse compression test results of the plywood with different thicknesses (9 and 12 mm) at different temperatures (25, −20, −65, −110, and −165 °C). At room temperature (25 °C) and low temperatures (−20 and −65 °C), most of the plywoods with 9 and 12 mm thicknesses exhibited an elastic behavior and fractured after reaching the ultimate stress. At cryogenic temperatures (−110 and −165 °C), most of

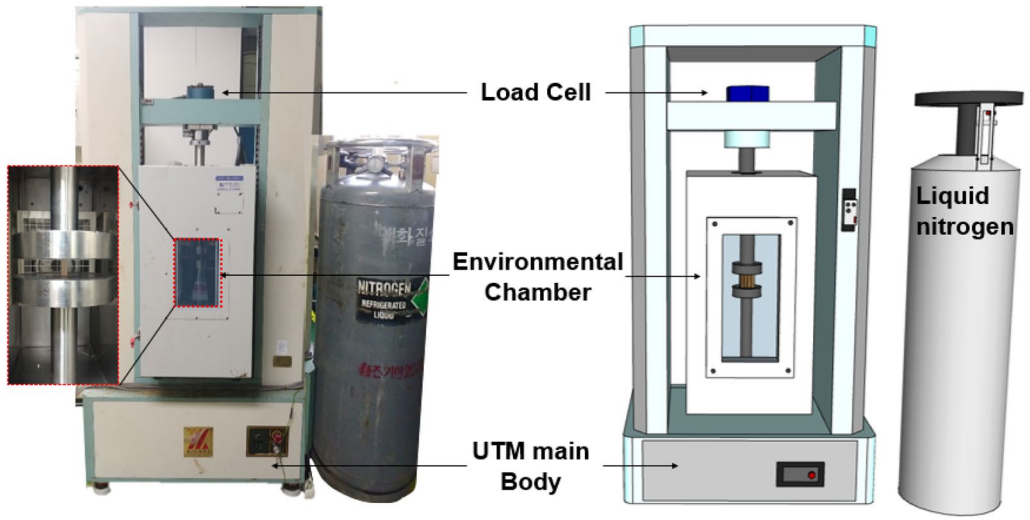

Fig. 5 Schematic diagram of the compression test machine

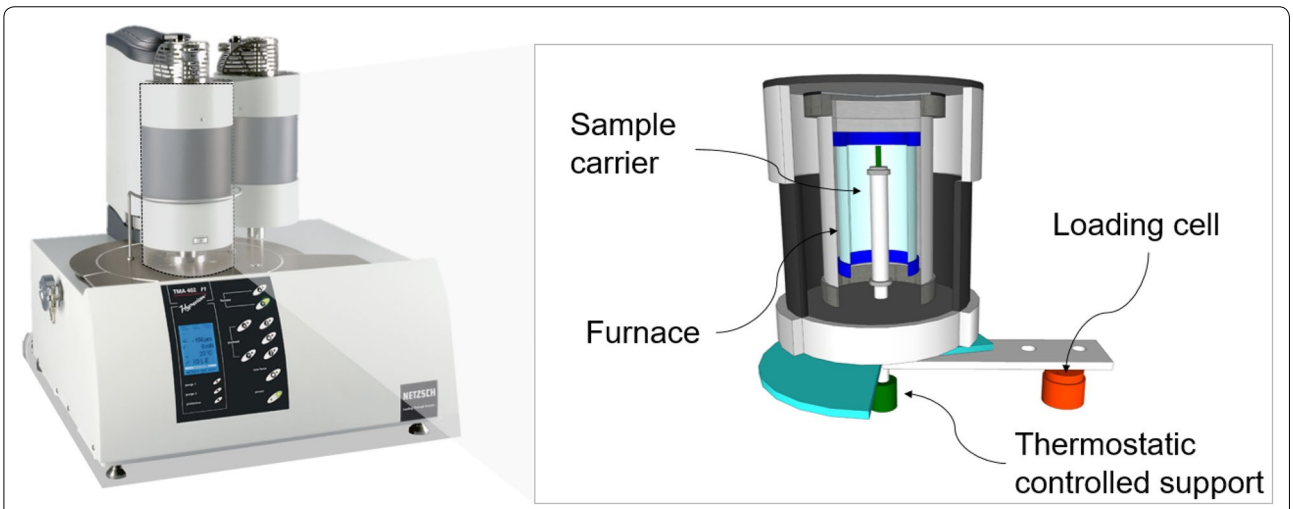

Fig. 6 Schematic diagram of TMA

the plywoods with 9 and 12 mm thicknesses exhibited a linear section and fractured with little plastic behavior. In summary, the plywood exhibited brittle characteristics in the longitudinal and transverse test directions at cryogenic temperatures (− 110 and − 165 °C).

Figure 8 shows the mean compressive strength and mean elasticity of the plywood specimens at room, low, and cryogenic temperatures based on Fig. 9 and Fig. 10. The calculation criterion for the mean compressive strength and elastic modulus in the longitudinal and transverse directions is as follows. The compressive strength was calculated from the ultimate strength of fracture before or near the yield point and from the strength of brittle fracture, as shown in Fig. 11 [25].

The experimental data were extracted with an error range of ± 10%. From the viewpoint of plate thickness, the compressive strength and elastic modulus of the plywood specimens with 9 and 12 mm thicknesses showed similar trends. With a decrease in temperature from room temperature to cryogenic temperatures, the compressive strength and elasticity increased. It has been reported that this phenomenon is highly influenced by water absorption and the ice crystals present in the wood cells, which absorb moisture at low temperatures. In addition, the adhesion strength increased, showing resistance to deformation at low temperatures [26–28].

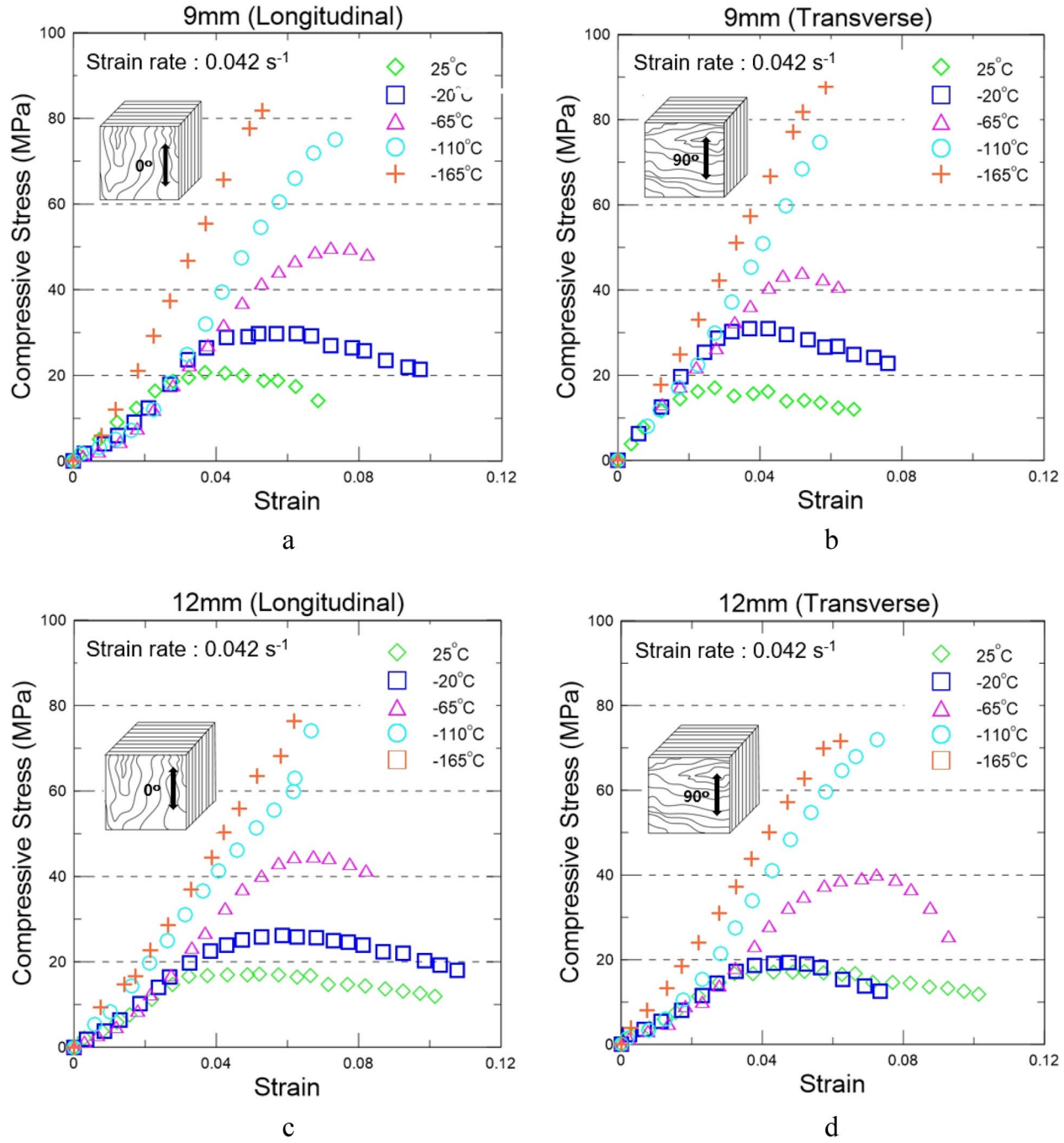

Fig. 7 Compressive test results of plywood specimens in longitudinal fiber direction for **a** 9 mm and in transverse fiber direction for **b** 9 mm thicknesses and in longitudinal fiber direction for **c** 9 mm and in transverse fiber direction for **d** 12 mm thicknesses

Mechanical performance: vertical direction

Figure 12 shows the compression test results of the plywood specimens of varying thicknesses (9 and 12 mm) in the vertical fiber direction at different temperatures (25, −20, −65, −110, and −165 °C). Compared with the plywood with longitudinal and transverse fiber directions, the plywood with vertical fiber direction showed different characteristics. For the plywood with vertical fiber direction, the stress–strain curves show linear elastic and plastic regions at temperatures between 25 and

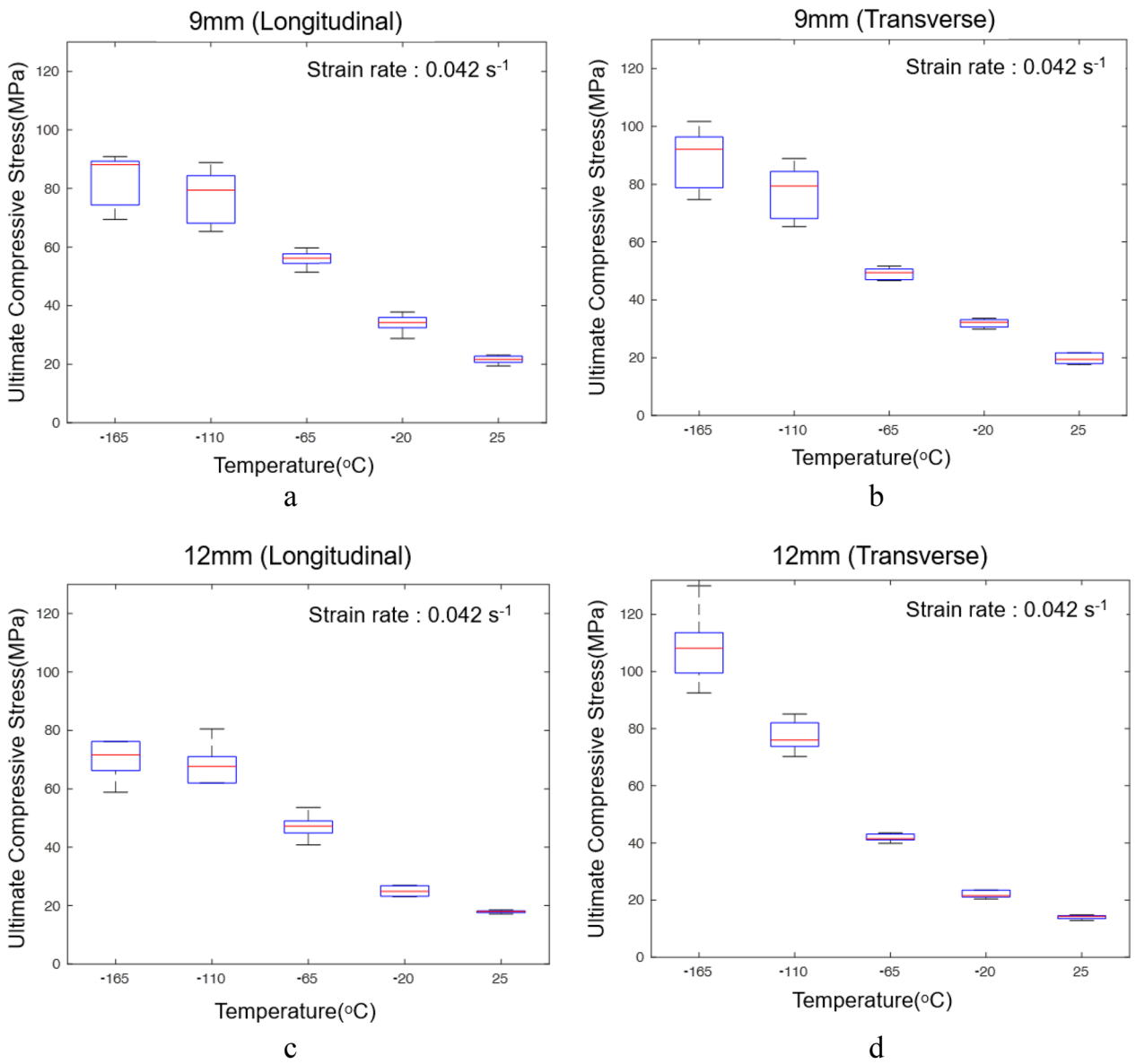

Fig. 8 **a** Average compressive strength and **b** average modulus of elasticity of plywood in longitudinal and transverse fiber directions

−110 °C. The yield strength increased with decreasing temperature. However, at −165 °C, the yield point is hard to distinguish. In addition, the plywood broke immediately without plastic deformation. Thus, the plywood shows brittle characteristics at −165 °C.

Figure 15 shows the average compressive strength and modulus of elasticity of the plywood specimens in the vertical direction at ambient (room), low, and cryogenic temperatures based on Fig. 13 and Fig. 14. The calculation criterion for the mean compressive strength and elastic modulus in the vertical direction is as follows. In the vertical direction, except at −165 °C, the offset yield strength is the stress that corresponds to a point at the intersection of a stress–strain curve and a line that is parallel to the specified elastic modulus line. This line is horizontally offset by a predetermined amount. The value of the offset (expressed as a percentage of strain) is 0.2% as defined by ISO 604. The yield strength is similar for the 9- and 12-mm thickness specimens, as shown in Fig. 15a. The 9- and 12-mm thickness specimens showed similar tendencies without significant differences in elastic modulus values. The 12-mm thickness specimen had a slightly higher value than the 9-mm thickness specimen did as temperature decreased. The elasticity modulus of

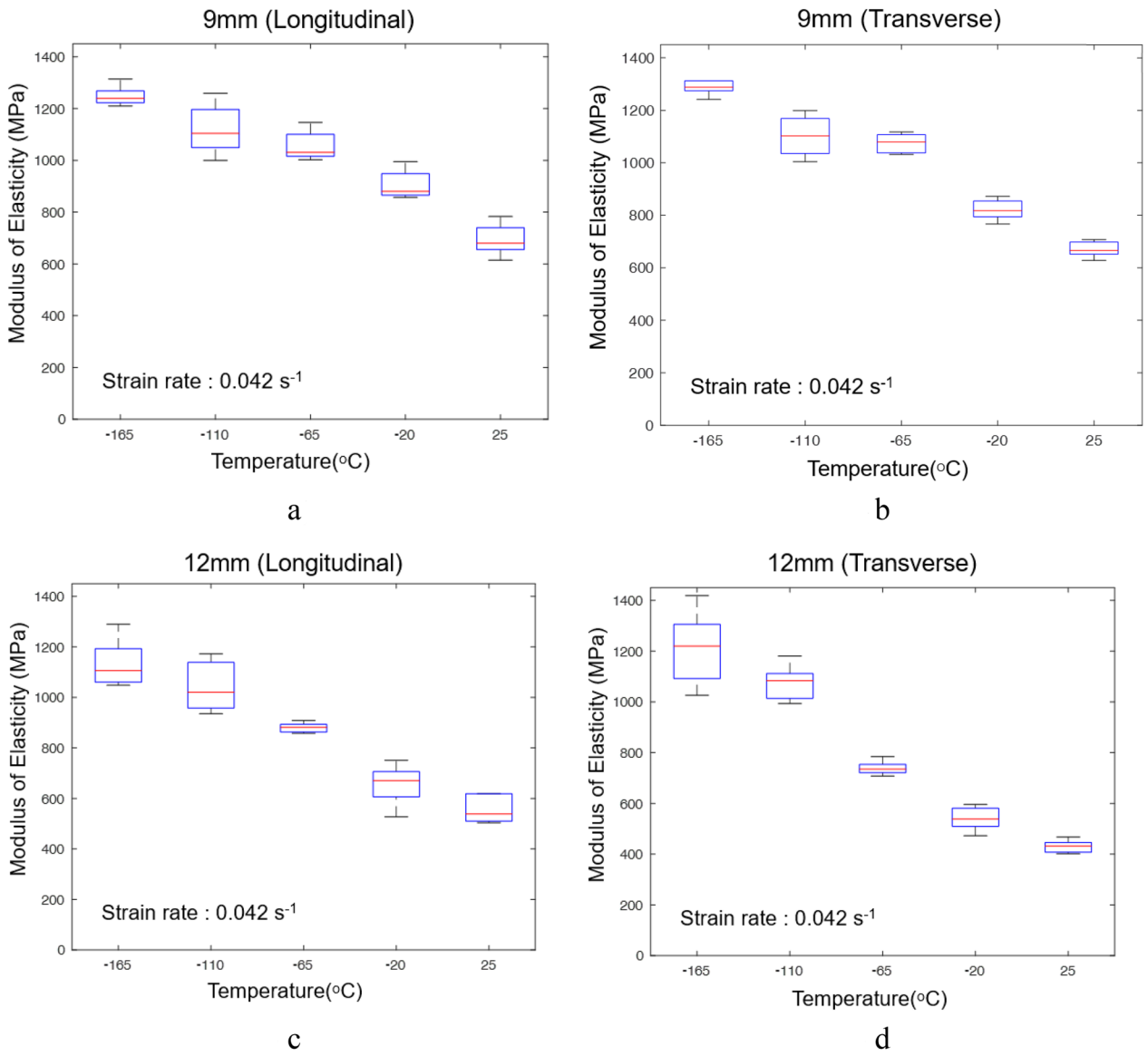

Fig. 9 **a**–**d** Average compressive strength of plywood in longitudinal and transverse fiber directions

the 9-mm thickness specimen was higher than that of the 12-mm thickness specimen at ambient temperature; however, the difference in elastic modulus between 9- and 12-mm thickness specimens increased with decreasing temperature, as shown in Fig. 15b.

With a decrease in temperature, the stiffness increases because of ice crystal formation below 0 °C. The hardening caused by ice crystal formation increases the elastic modulus, thereby preventing deformation [26, 27]. This is also because of the tendency of the resin to increase in strength as temperature decreases [9]. The 12-mm thickness specimen has more resin and more layers than the 9-mm thickness specimen does. Thus, although the difference between the 9 and 12-mm thickness specimens was small and the tendency was similar, the elastic modulus of the 12-mm thickness specimen was higher than that of the 9-mm thickness specimen at low and cryogenic temperatures, because of an increase in resin strength and ice crystal formation at low temperature. Therefore, in the design approach to Mark-III, 12t plywood should be used near the primary barrier exposed to cryogenic environments, while 9t plywood should be used near the inner hull exposed to ambient temperature. That is, if the 9t and 12t plywoods are designed differently according to

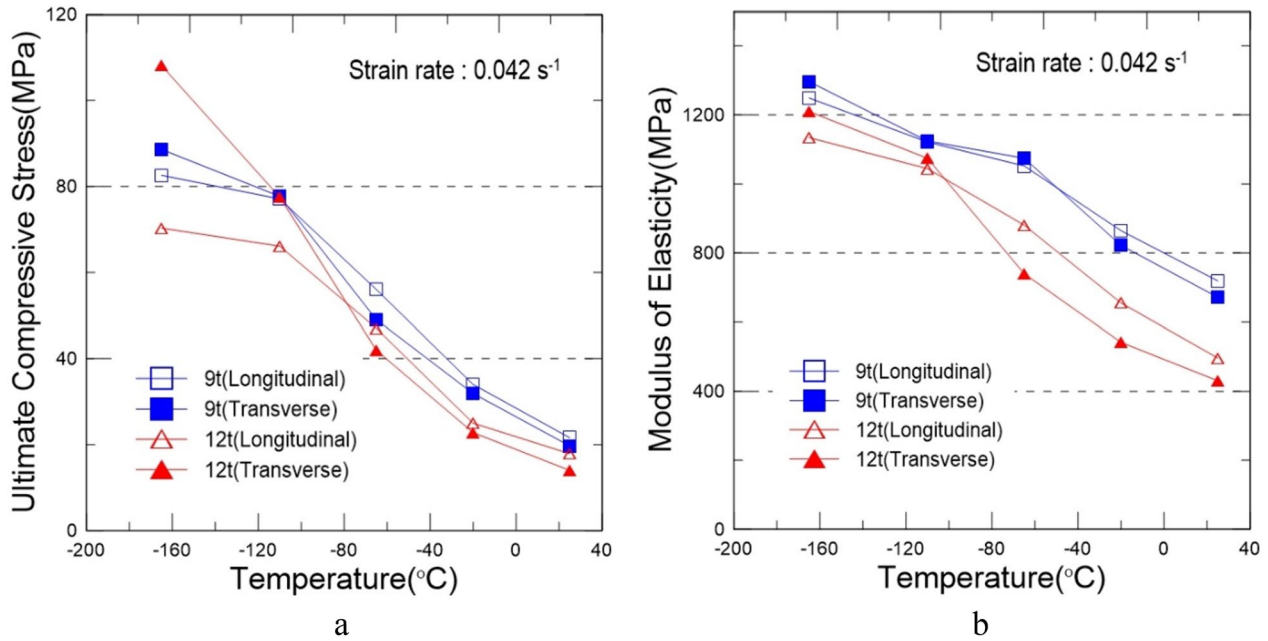

Fig. 10 **a**–**d** Average modulus of elasticity of plywood in longitudinal and transverse fiber directions

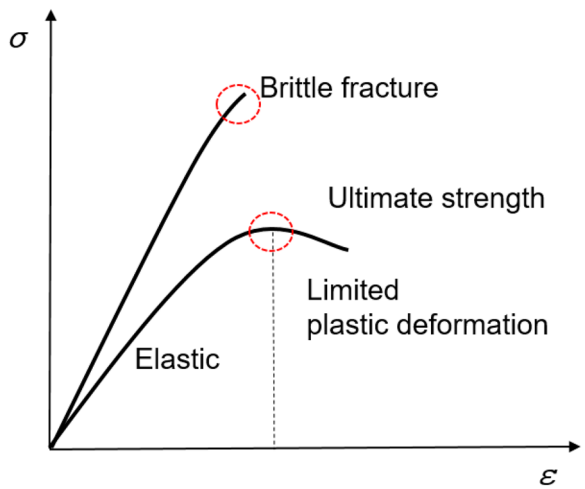

Fig. 11 Shape of the stress–strain curve in longitudinal and transverse directions

the temperatures of the environments to which they are exposed, the stiffness of the structure can be increased.

Macroscopic and microscopic observations

To investigate the effect of test temperature, fiber direction, and thickness on the fracture behavior of the plywood, macroscopic and microscopic analyses were conducted. In the present study, the fracture shapes in mainly the longitudinal and transverse directions were analyzed, because the fracture shapes in the vertical direction were almost the same regardless of temperature and thickness [10].

Figure 16 shows the macroscopic images of the tested plywood specimens. As can be seen, no noticeable macroscopic breakage occurred in the plywood specimens tested at temperatures between 25 and −20 °C. At temperatures below −65 °C, a well-marked macroscopic failure is observed with delamination and a transverse crack. Crack progression is clearly visible at cryogenic temperatures (−110 and −165 °C). Choi and Sankar reported the fracture toughness of a transverse crack in laminates at cryogenic temperatures and defined the damage progression in laminated composites such as micro-cracks, transverse cracks, delamination, and debonding of the facesheet [25]. The present study shows a similar trend of damage progression at cryogenic temperatures (−110 and −165 °C). It is thought that the fracture of the plywood at cryogenic temperatures is mainly due to the thermal contraction phenomenon, which occurred between the fibers with a decrease in temperature [26]. In addition, plywood is a material manufactured from thin layers of wood veneer that are glued to adjacent layers, unlike solid wood. Thus, the contraction of resin at the low temperature causes micro-cracks because of the difference in thermal contraction between resin and wood fiber at low temperature [28]. Moreover, PF resin is reported to have good temperature stability; however, for MUF

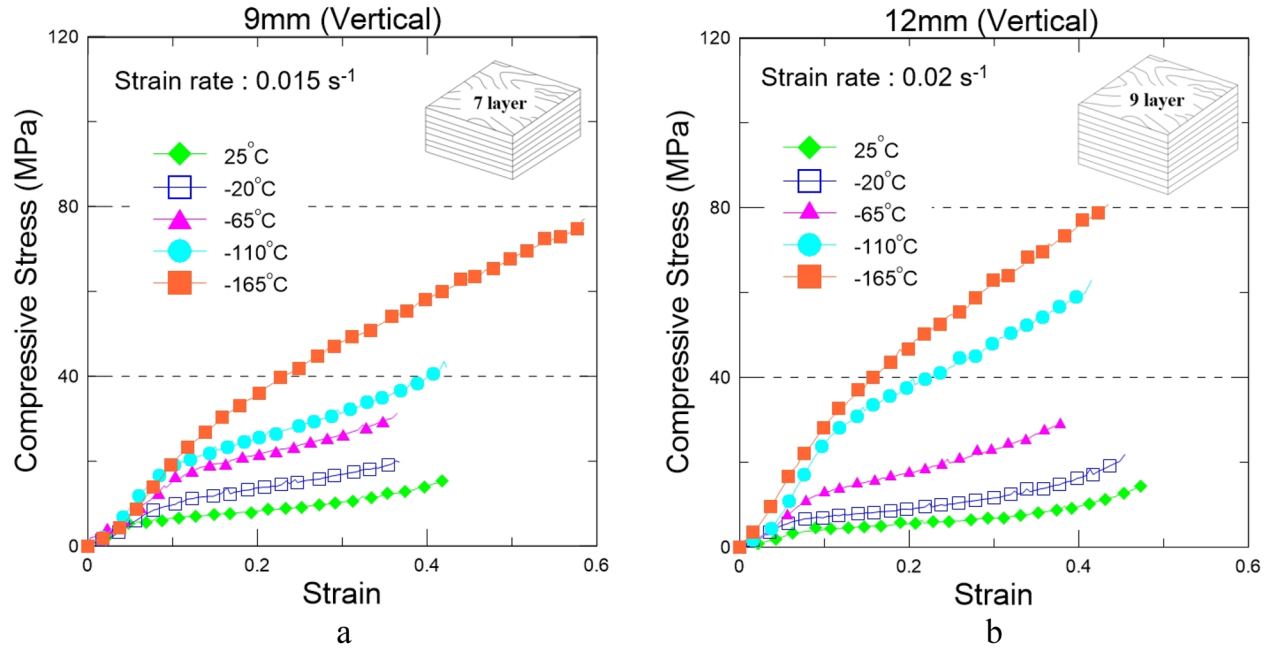

Fig. 12 Compression test results of plywood specimens in vertical fiber direction for **a** 9 mm and **b** 12 mm thicknesses

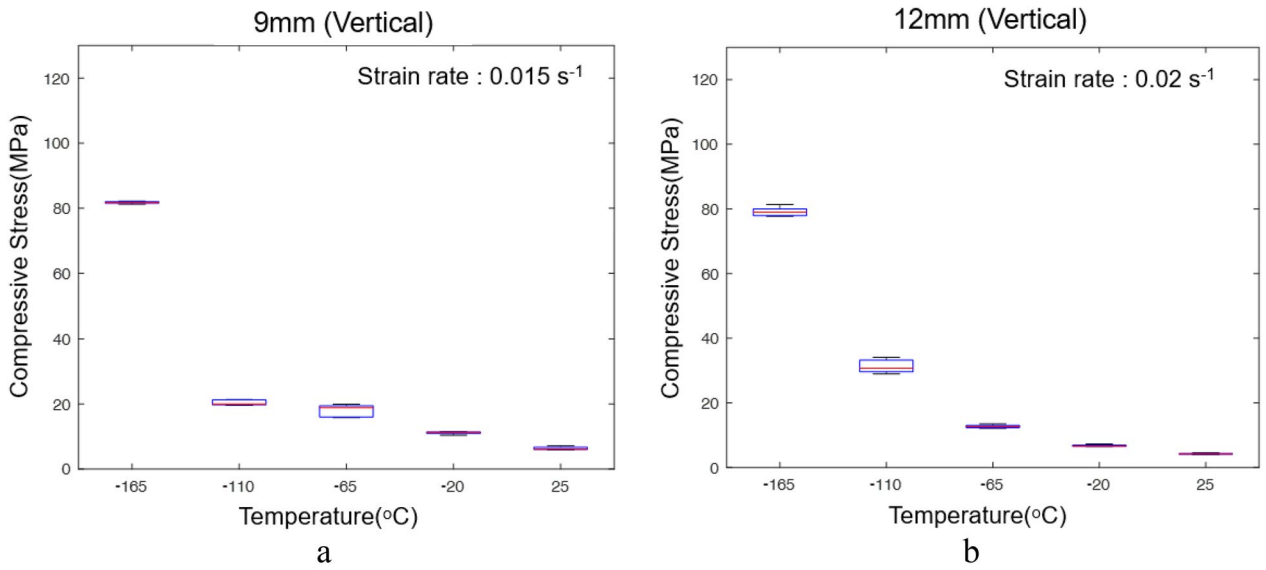

Fig. 13 **a**, **b** Average compressive strength of plywood in the vertical fiber directions

resin, the extent of cracking is significant due to a reduction in temperature stability [28].

Following the macroscopic observation, microscopic observation was conducted by scanning electron microscopy (SEM) to confirm the crack growth characteristics of the tested samples. The identification of micro-cracks and prediction of cracks are crucial for sandwich-layered structures such as plywood. Figure 17 shows the SEM images of the tested samples. As can be seen in Fig. 17a, crack propagation occurs with a decrease in temperature from 25 to −65 °C with the initiation of micro-cracks in the transverse direction [29]. As the temperature decreases to −110 °C, the large thermal contraction causes transverse cracks

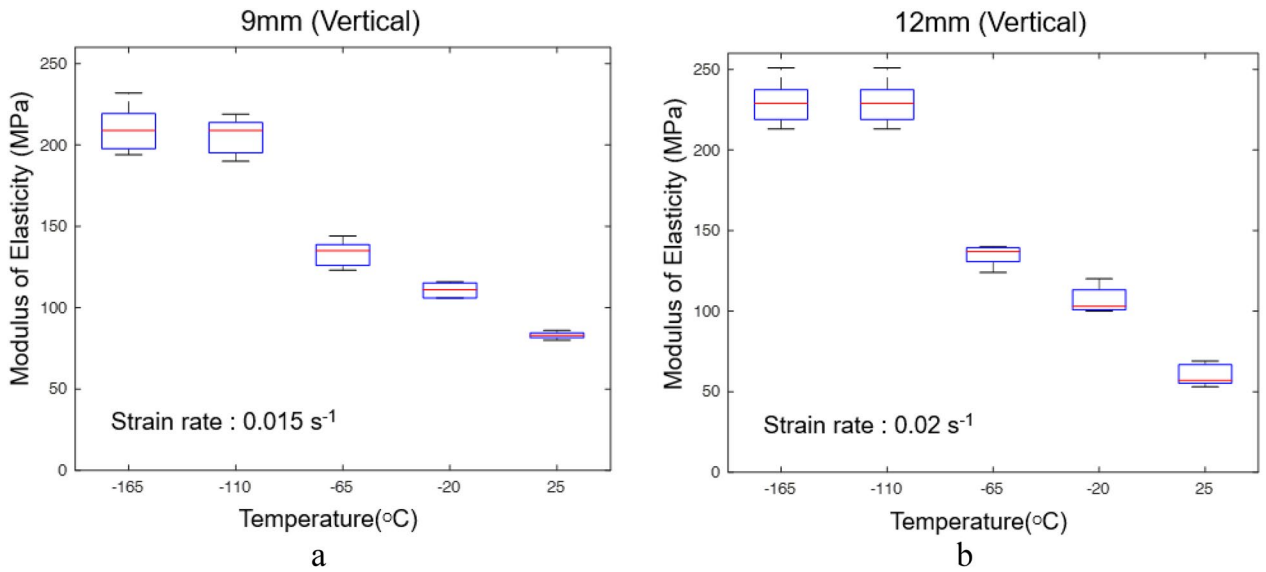

Fig. 14 **a**, **b** Average modulus of elasticity of plywood in the vertical fiber directions

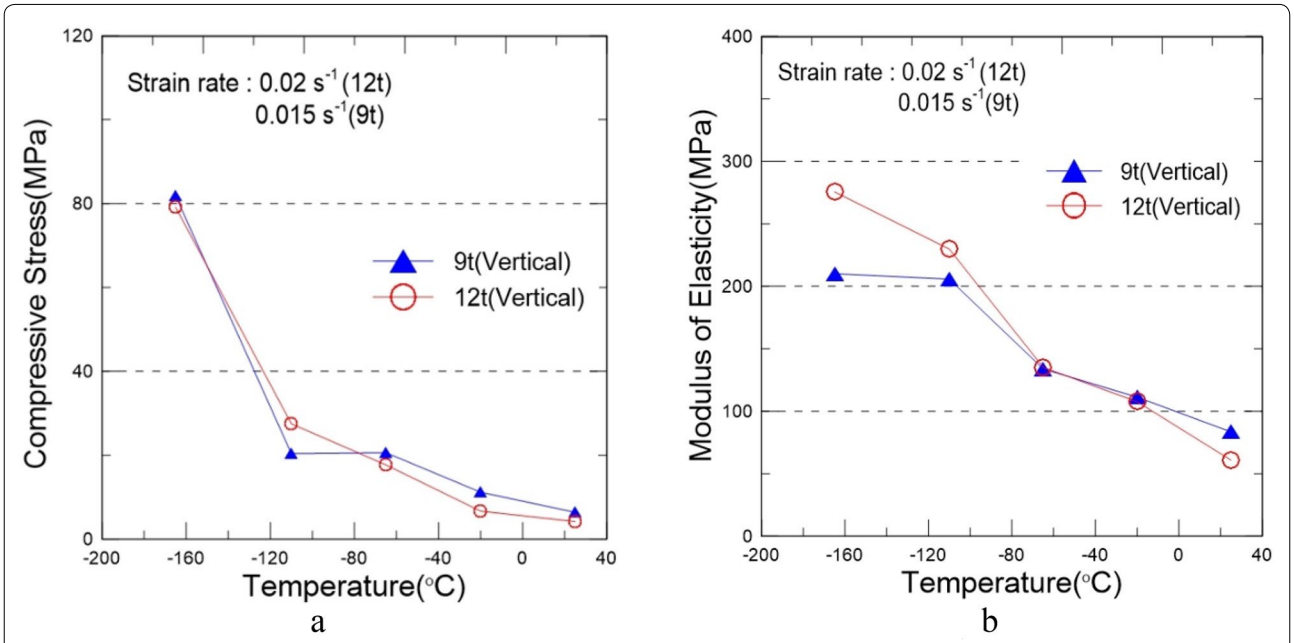

Fig. 15 **a** Average compressive strength and **b** average modulus of elasticity of plywood in the vertical direction

and delamination (Fig. 17b). This leads to an interfacial crack in the adjacent layer at − 165 °C, as shown in Fig. 17c. It can be said that the phenomenon of microcrack and interfacial crack formation is a major issue in LNG CCSs along with the risk of cryogenic liquid spillage that can cause the fracture of sandwich structures.

Ultimate strain analysis

The mechanical properties of plywood such as ductility and brittleness were confirmed from the stress–strain curves shown in Fig. 7. Based on this, the ultimate strain of plywood was determined, and is shown in Fig. 18. In the present study, the fracture characteristics

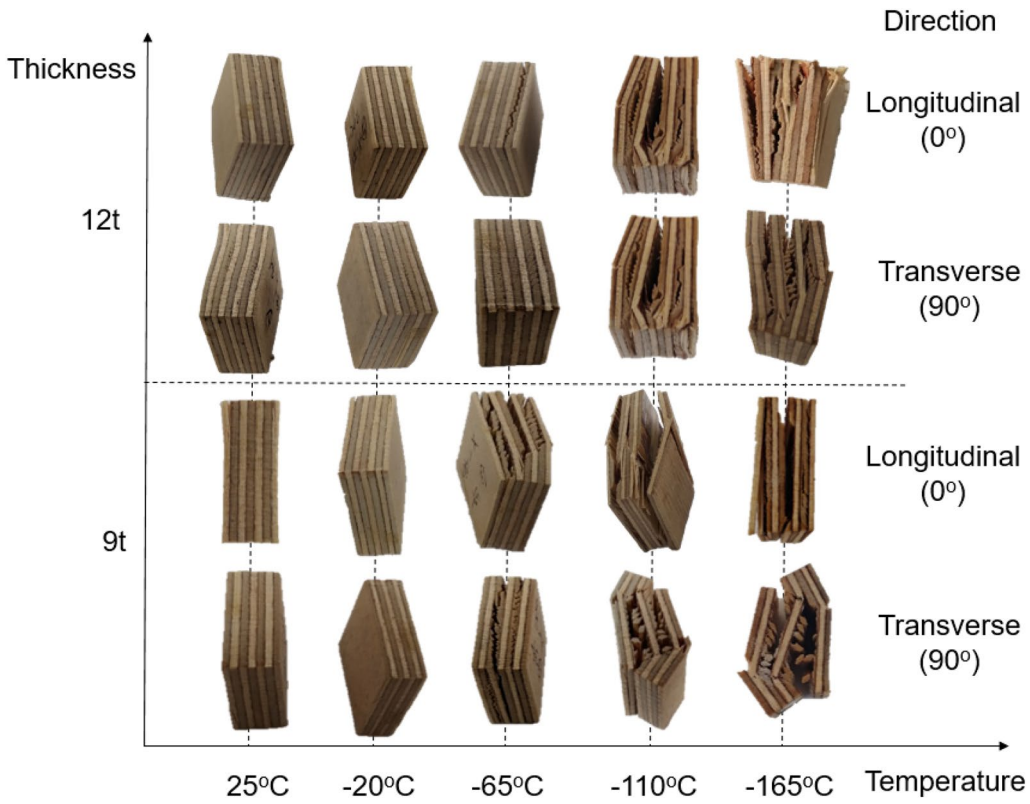

Fig. 16 Macroscopic images showing fracture characteristics of MUF plywood specimens

of the plywood were determined from its mechanical properties in the longitudinal and transverse directions, as shown in Fig. 18 based on Fig. 7. With a decrease in temperature, a micro-crack occurred due to the thermal contraction effect. With the growth of micro-crack, fracture occurred with crack propagation. Therefore, the extent of crack growth can be determined from the ultimate fracture characteristics.

Figure 18 shows the temperature-dependent ultimate strain behaviors of the 9 and 12-mm thickness plywood specimens in longitudinal and transverse directions. As shown, the ultimate strain increases with a decrease in temperature; however, at − 110 °C, the ultimate strain remained the same or slightly decreased. This indicates that degradation started at a critical temperature of − 110 °C because the ultimate strain is the fracture strain caused by the brittle characteristics of plywood at − 110 °C. As shown in Fig. 17, the crack propagation trends are similar at − 110 °C and − 165 °C. This allowed us to determine the structural characteristics of the laminated wood from the critical temperature of − 110 °C for the mechanical properties.

Thermal expansion coefficient

To investigate the temperature-dependent thermal expansion coefficient of the plywood, TMA was performed in the longitudinal and transverse directions, which are the loading directions. Figure 19 shows the temperature-dependent thermal expansion coefficient of the plywood specimens in the longitudinal and transverse fiber directions. The thermal contraction in the transverse direction was higher than that in the longitudinal direction from 25 to − 110 °C. This is because a transverse crack occurs at the fiber layer with 90° fibers at ambient temperature (25 °C) and low temperatures (− 20 and − 65 °C), as shown in Fig. 17. The thermal contraction is higher in the transverse direction because it has more layers of 90° fibers than the longitudinal direction does. However, the thermal contraction in the transverse direction was similar to that in the longitudinal direction below − 110 °C. As shown in Fig. 16 and Fig. 17, interfacial cracks occur in 0° fibers and transverse cracks occur in 90° fibers at cryogenic temperatures (− 110 °C and − 165 °C). All the layers including 0° and 90° fibers have cracks regardless

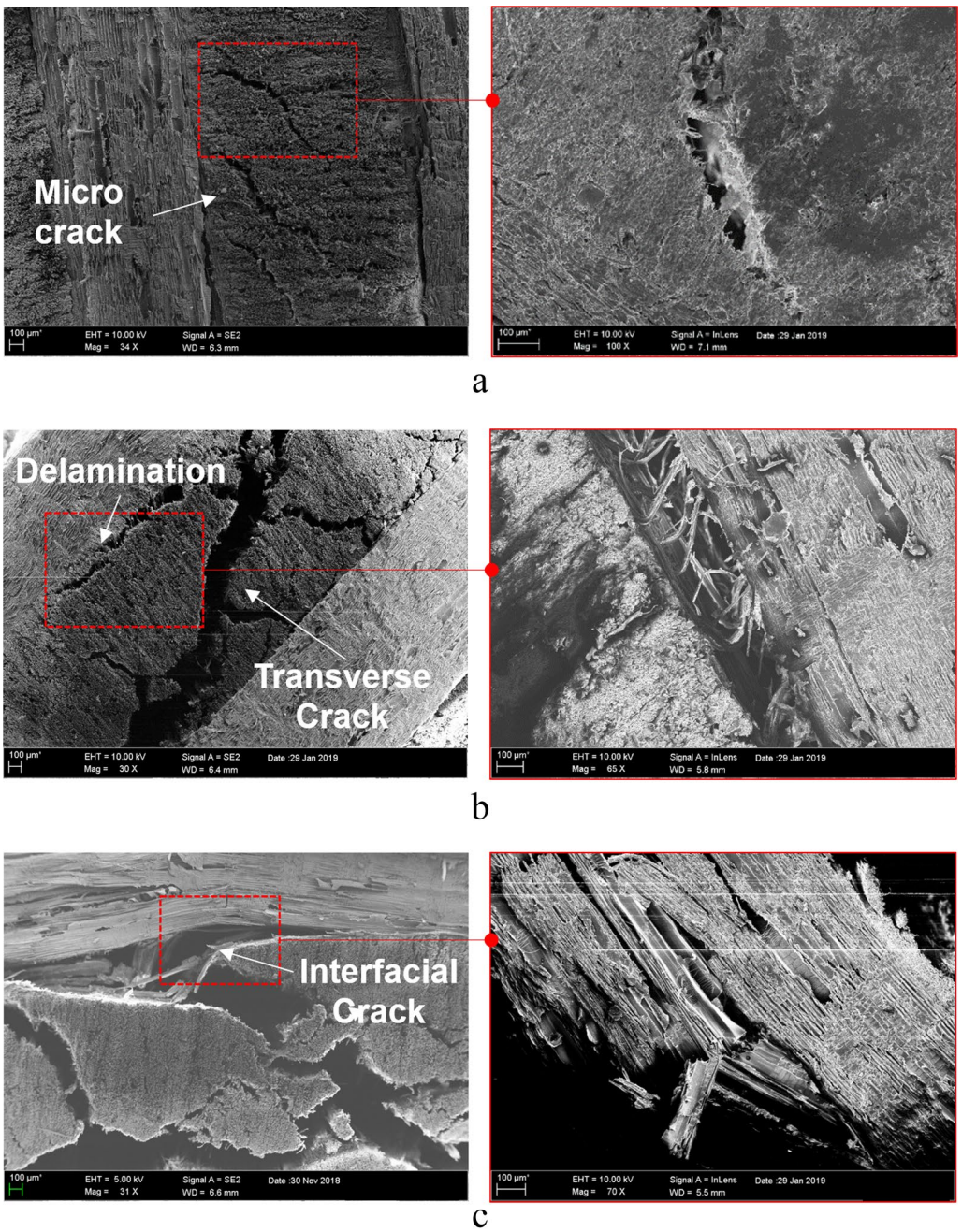

Fig. 17 SEM images of plywood specimens at different temperature regimes: **a** ambient temperature and low temperature, **b** low temperature and cryogenic temperature, and **c** cryogenic temperature

of the fiber direction. According to these phenomena, at − 110 °C, the fracture shape and thermal contraction are similar. Thus, in the design of LNG CCSs, the use of plywood in the longitudinal direction would be better from the viewpoint of structural safety since the thermal contraction is lower in the longitudinal direction than in the transverse direction.

In Fig. 19, it can be seen that the thermal expansion coefficient converges around a certain temperature. The convergence of the thermal expansion coefficient implies that the material does not shrink or expand anymore; however, breakage is more likely to occur due to external forces. The present study defines the convergence temperature of the curve as the critical

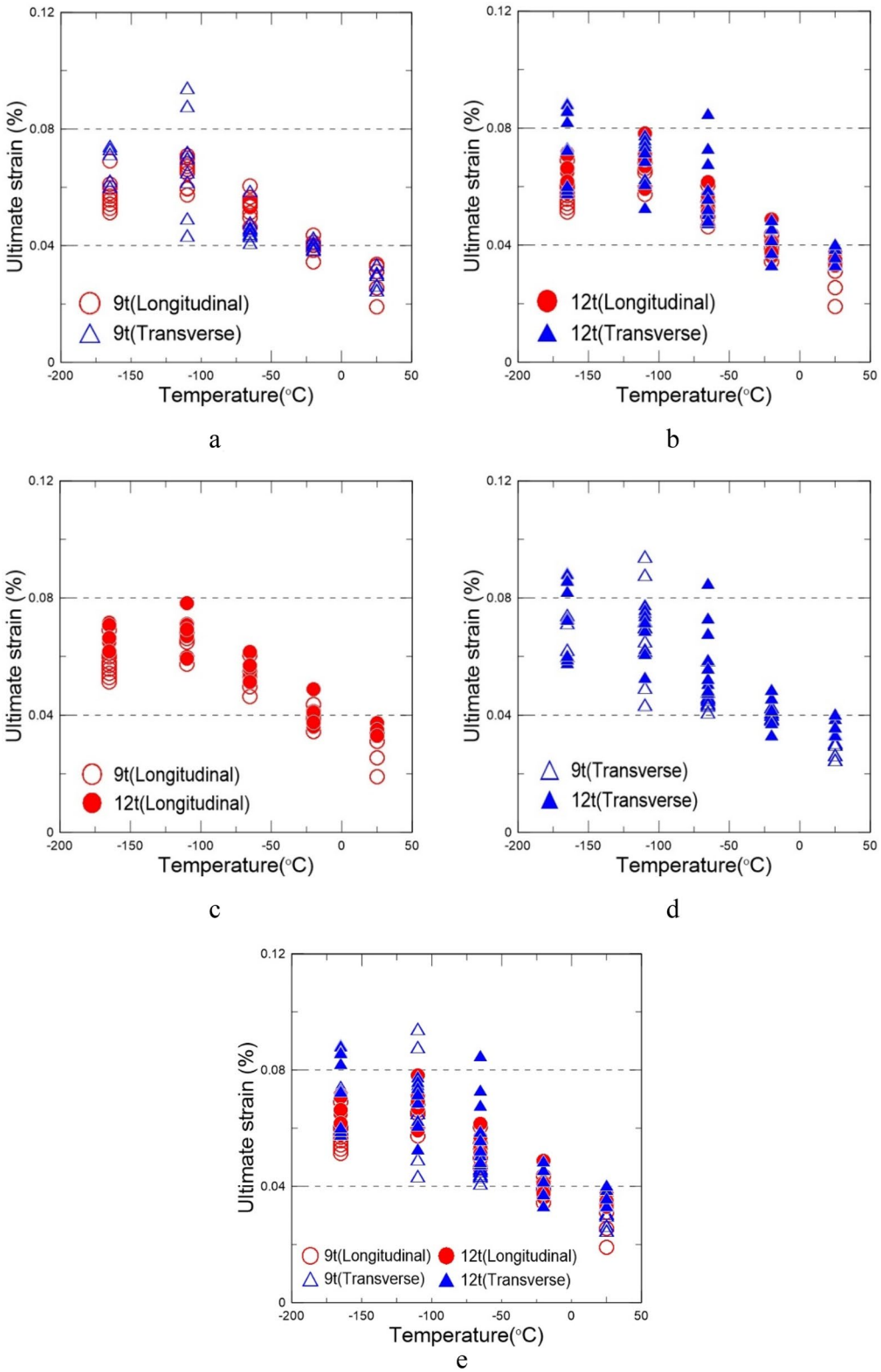

Fig. 18 Ultimate strain of 9t and 12t plywoods in longitudinal and transverse fiber directions: **a** 9t, **b** 12t, **c** longitudinal fiber direction, **d** transverse fiber direction, and **e** overall graph

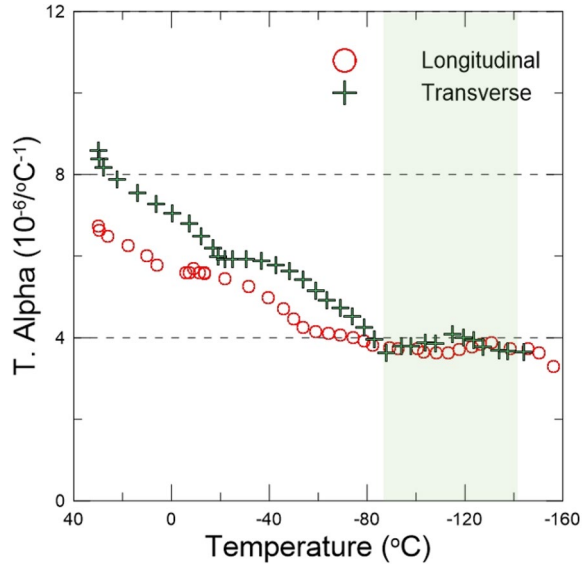

Fig. 19 Thermal expansion coefficient of plywood

temperature at which the transition from ductility to brittleness occurs. This critical temperature is abbreviated as "CT". From Fig. 19, it is confirmed that the CT of the MUF resin plywood is approximately − 110 °C.

The CT is important because when a structural material is exposed to a cryogenic liquid, the material becomes brittle, which can be dangerous from the viewpoint of structural safety. In other words, the transition to brittleness causes mechanical degradation of plywood, which serves as a strong frame and distributes the local load. In addition, the fiber direction, which is most affected by the CT, should be considered an important design parameter for NO96 plywood box and the plywood wall plate of Mark-III because the thermal contraction is higher in the transverse direction than in the longitudinal direction at ambient and low temperatures. It is important to predict the types of fractures, such as ductile fracture and brittle fracture, of plywood depending on the temperature in the design of LNG CCSs to ensure structural stability. In this study, the CT was determined by both mechanical and thermal analyses, and was found to be − 110 °C for MUF resin plywood.

This implies that the MUF resin plywood requires extra consideration for impacts of over 79 MPa. However, MUF resin plywood can be applied to LNG CCSs because it can sufficiently withstand sloshing impact since its strength is higher than the required strength of 65 MPa at a cryogenic temperature, as specified by DNV GL [16, 30].

Conclusion

In this study, compression tests were conducted on MUF resin plywood used in LNG CCSs with different plywood thicknesses, fiber orientations, and test temperatures. The following conclusions are drawn from the obtained results:

- The mechanical characteristics of the MUF resin plywood used in LNG CCSs were determined in the longitudinal and transverse directions as well as vertical fiber direction. The mechanical properties such as yield strength and elastic modulus increased with decreasing temperature.
- The elastic modulus of the 9t plywood is higher than that of the 12t plywood at ambient temperature. However, the elastic modulus of the 12t plywood is higher than that of the 9t plywood at cryogenic temperatures. This indicates that 9t and 12t plywoods can be applied to LNG CCSs depending on the temperature.
- At temperatures below − 65 °C, macroscopic failure, such as delamination and transverse crack, was observed. At cryogenic temperatures (− 110 and − 165 °C), crack progression was clearly visible. The cracks were observed in detail by SEM.
- For the longitudinal and transverse compression tests, the plywood exhibited abrupt brittle characteristics at temperatures below − 110 °C. The ultimate strain increased with decreasing temperature; however, at − 110 °C, the ultimate strain was the same or slightly decreased.
- In this study, the CT was determined by both mechanical and thermal analyses. The thermal expansion curve exhibited a convergence region, and the CT of the MUF resin plywood was found to be − 110 °C.

The findings of the present study provide important insights into the low-temperature brittleness of MUF resin plywood, which can aid in the design of LNG CCSs using MUF resin plywood from the viewpoint of structural safety at low and cryogenic temperatures. Furthermore, the results of the thermal contraction experiment revealed that the longitudinal loading direction has higher stiffness than the transverse direction does, and is thus suitable for the design of a plywood box of NO96 and a plywood wall plate of Mark-III. From the design perspective, it is considered that MUF resin plywood can be used in LNG CCSs depending on the temperature since this study verified the reliability of MUF plywood regarding its low-temperature brittleness at a CT derived by thermomechanical analysis.

Abbreviations
MUF: Melamine–urea–formaldehyde; LNG: Liquefied natural gas; CCSs: Cargo containment systems; PUF: Polyurethane foam; FEA: Finite element analysis; UTM: Universal testing machine; TMA: Thermomechanical analysis; SEM: Scanning electron microscopy; CT: Critical temperature; MT: Million tons; PF: Phenolic-formaldehyde; GTT: Gaztransport & Technigaz.

Acknowledgements
This work was supported by the R&D Platform Establishment of Eco-Friendly Hydrogen Propulsion Ship Program (No. 20006644) funded by the Ministry of Trade, Industry & Energy (MOTIE, Korea). This work was supported by the National Research Foundation of Korea (NRF) grant funded by the Ministry of Science and ICT (MSIT) (No. 2018R1A2B6007403). This research was funded and conducted under "the Competency Development Program for Industry Specialists" of the Korean Ministry of Trade, Industry and Energy (MOTIE), operated by Korea Institute for Advancement of Technology (KIAT) (No. P0001968, The Competency Development Program for Industry Specialist).

Authors' contributions
SJC performed the compression test, and was a major contributor in writing the manuscript. JDK was a co-performer of the test. HKO, YTK and SBP contributed to the interpretation of the data. SKK optimized experimental setup for compression test and performed the research for analyzing data. JHK contributed to reviewing the original manuscript. JML supervised the experiments and contributed reviewing the original manuscript. All authors read and approved the final manuscript.

Funding
This work was supported by the R&D Platform Establishment of Eco-Friendly Hydrogen Propulsion Ship Program (No. 20006644) funded by the Ministry of Trade, Industry & Energy (MOTIE, Korea). This work was supported by the National Research Foundation of Korea (NRF) grant funded by the Ministry of Science and ICT (MSIT) (No. 2018R1A2B6007403). This research was funded and conducted under "the Competency Development Program for Industry Specialists" of the Korean Ministry of Trade, Industry and Energy (MOTIE), operated by Korea Institute for Advancement of Technology (KIAT). (No. P0001968, The Competency Development Program for Industry Specialist)

Availability of data and materials
Data generated in this study are not available.

Competing interests
The authors declare that they have no competing interests.

Author details
[1] Department of Naval Architecture and Ocean Engineering, Pusan National University, Jangjeon-Dong, Geumjeong-Gu, Busan 609-735, South Korea.
[2] Hyundai Heavy Industries Co., Ltd, Jeonha-dong, Dong-Gu, Ulsan 44032, South Korea.

Received: 10 October 2019 Accepted: 5 April 2020
Published online: 16 April 2020

References
1. Dobrota Đ, Lalić B, Komar I (2013) Problem of boil-off in LNG supply chain. Trans Marit Sci 2(02):91–100
2. Paunov VN (2003) Novel method for determining the three-phase contact angle of colloid particles adsorbed at air-water and oil-water interfaces. Langmuir 19(19):7970–7976
3. Choi SW, Roh JU, Kim MS, Il Lee W (2012) Analysis of two main LNG CCS (cargo containment system) insulation boxes for leakage safety using experimentally defined thermal properties. Appl Ocean Res 37:72–89
4. Grexa O, Horváthová E, Bešinová O, Lehocký P (1999) Flame retardant treated plywood. Polym Degrad Stab 64(3):529–533
5. Kim JH, Park DH, Lee CS et al (2015) Effects of cryogenic thermal cycle and immersion on the mechanical characteristics of phenol-resin bonded plywood. Cryogenics 72:90–102
6. Ayrilmis N, Buyuksari U, As N (2010) Bending strength and modulus of elasticity of wood-based panels at cold and moderate temperatures. Cold Reg Sci Technol 63(1–2):40–43
7. Demirkir C, Özsahin Ş, Aydin I, Colakoglu G (2013) Optimization of some panel manufacturing parameters for the best bonding strength of plywood. Int J Adhes Adhes 46:14–20
8. Goodrich T, Nawaz N, Feih S et al (2010) High-temperature mechanical properties and thermal recovery of balsa wood. J Wood Sci 56(6):437–443
9. Kim JH, Choi SW, Park DH et al (2018) Effects of cryogenic temperature on the mechanical and failure characteristics of melamine–urea–formaldehyde adhesive plywood. Cryogenics 91:36–46
10. Arswendy A, Moan T (2015) Strength and stiffness assessment of an LNG containment system-crushing and buckling failure analysis of plywood components. Eng Fail Anal 48:247–258
11. Choi SW, Li M, Lee WI, Kim HS (2014) Analysis of buckling load of glass fiber/epoxy-reinforced plywood and its temperature dependence. J Compos Mater 48(18):2191–2206
12. Mohd Yusof N, Md Tahir P, Lee SH et al (2019) Mechanical and physical properties of cross-laminated timber made from *Acacia mangium* wood as function of adhesive types. J Wood Sci 65(1):20
13. Kijidani Y, Morita H, Aratake S et al (2019) Partial compression strength of sugi (Japanese cedar, *Cryptomeria japonica*) wood near the pith perpendicular to the grain. J Wood Sci 65(1):16
14. No BY, Kim MG (2004) Syntheses and properties of low-level melamine-modified urea-melamine-formaldehyde resins. J Appl Polym Sci 93(6):2559–2569
15. Det Norske Veritas AS (2005) Fatigue design of offshore steel structures
16. Graczyk M, Moan T (2008) A probabilistic assessment of design sloshing pressure time histories in LNG tanks. Ocean Eng 35(8–9):834–855
17. Yu YH, Kim BG, Lee DG (2013) Cryogenic reliability of the sandwich insulation board for LNG ship. Compos Struct 95:547–556
18. Park YIL, Lee JH (2018) Buckling strength of GTT NO96 LNG carrier cargo containment system. Ocean Eng 154:43–58
19. Kim MH, Kil YP, Lee JM, Chun MS, Suh YS, Kim WS, Noh BJ, Yoon JH, Kim MS, Urm HS (2011) Cryogenic fatigue strength assessment for MARK-III insulation system of LNG carriers. J Offshore Mech Arct Eng 133(4):041401–041411
20. Kuo JF, Campbell RB, Ding Z et al (2009) LNG tank sloshing assessment methodology-the new generation. Int J Offshore Polar Eng 19:241–253
21. EN 324-1 (1993) Wood-based panels. Determination of dimensions of boards. Part 1: determination of thickness, width and length. European Committee for Standardization (CEN), Brussels
22. EN 315 (2000) Plywood. Tolerances for dimensions. European Committee for Standardization (CEN), Brussels
23. ISO 7726 (1998) Ergonomics of the thermal environment, instruments for measuring physical quantities. International Organization for Standardization (ISO), Geneva
24. ASTM E831–14 (2014) Standard test method for linear expansion of solid materials by thermomechanical analysis. American Society for Testing and Materials, West Conshohocken
25. Rösler J, Harders H, Bäker M (2007) Mechanical behaviour of engineering materials: metals, ceramics, polymers, and composites. Springer Science & Business Media, Berlin
26. Ogan JADL (1999) Adjusting modulus of elasticity of lumber for changes in temperature. For Prod J 49(10):82–94
27. Bekhta P, Marutzky R (2007) Bending strength and modulus of elasticity of particleboards at various temperatures. Holz als Roh und Werkst 65(2):163–165
28. Moubarik A, Pizzi A, Allal A, Charrier F, Charrier B (2009) Cornstarch and tannin in phenol-formaldehyde resins for plywood production. Ind Crops Prod 30(2):188–193
29. Choi S, Sankar BV (2007) Fracture toughness of transverse cracks in graphite/epoxy laminates at cryogenic conditions. Compos Part B Eng 38(2):193–200
30. Det Norske Veritas (2006) Sloshing analysis of LNG membrane tanks. DNV Classif Notes 30(9):49

Publisher's Note